J. Microbiol. Biotechnol. (2006), **16**(1), 109–117

JOURNAL OF MICROBIOLOGY AND BIOTECHNOLOGY

Studies on the Binding Affinity of Aminoglycoside Antibiotics to the HIV-1 Rev Responsive Element for Designing Potential Antiviral Agents

KWON, YOUNGJOO*

College of Pharmacy, Ewha Womans University, Seoul 120-750, Korea

Received: August 4, 2005
Accepted: October 1, 2005

Abstract The Rev binding to Rev Responsive Element (RRE) of HIV-1 mRNA plays an important role in the HIV-1 viral replication cycle. The disruption of the Rev-RRE interaction has been studied extensively in order to develop a potential antiviral drug. In order to provide the basis for a more promising approach to develop a Rev-RRE binding inhibitor against HIV-1 infection, it is necessary to understand the binding modes of the aminoglycoside antibiotics to RRE. In the present study, the binding mode of a modified antibiotic, a neamine conjugated with pyrene and arginine (NCPA), to RRE has been studied by the methods of T_m measurement and spectroscopic analysis of RRE with or without antibiotics. The results confirmed that NCPA competes with Rev in binding to RRE.

Key words: Aminoglycoside antibiotics, HIV-1 RRE, binding affinity to RRE, inhibition of HIV-1 Rev-RRE interaction, T_m

Human immunodeficiency virus type 1 (HIV-1) was identified as a causative species for Acquired Immunodeficiency Syndrome (AIDS) in the early 1980s [1, 34]. Since this discovery, diverse efforts in the areas of biology, biochemistry, and structural biology have been conducted to control AIDS. One of these results is the discovery of the HIV-1 viral replication cycle that requires the expression of two classes of viral mRNA. The early class of HIV-1 transcripts is multispliced and encodes viral regulatory proteins, such as Trans Activator of Transcription (Tat) and Regulator of Expression of Virion (Rev) proteins, and the late class of HIV-1 mRNA is nonspliced or singly-spliced and results in viral structural proteins, including Gag-Pol and Env [34, 36]. These viral structural proteins are required for the assembly of infectious virion. Rev has two important roles in the HIV-1 viral replication cycle: First, the translated Rev protein, formed via the early transcript, initiates inhibition of the Tat expression when Rev reaches the threshold level concentration. Second, Rev regulates the viral RNA transport from nucleus to cytoplasm through binding to a highly structured RNA element, RRE. This Rev binding to RRE inhibits the spliceosome complex formation on the late HIV-1 mRNAs, leading to nonspliced or singly-spliced viral RNA [7, 21]. These properties together with the interaction between Rev and RRE of HIV-1 have been the focus for the most promising potential target of the therapeutic intervention of the HIV-1 replication. In addition, it has been experimentally proven that the replication of HIV-1 retrovirus is abolished when the Rev-RRE interaction is absent. Therefore, the intervention of the Rev-RRE interaction has been studied toward the aim of developing a potential antiviral drug [6, 8, 13, 26, 38]. In previous studies, it was discovered that certain aminoglycoside antibiotics (Fig. 1), such as neomycin, compete with the Rev for binding to the RRE stem-loop IIB domain *in vitro*. They also interfere with Rev function *in vivo*, thereby inhibiting the production of the HIV-1 virus [16, 17, 35]. The molecular mechanism of how the aminoglycosides bind to the RRE construct and prevent the binding of the Rev peptide is still under intensive examination [17]. Recently, it has been suggested that the recognition of aminoglycosides might be dependent on the secondary folding structure of the RNA rather than its specific sequence [11]. The most potential Rev-binding inhibitor, neomycin, is capable of nonspecific binding to the RRE stem-loop IIB core with a 3:1 stoichiometric coefficient of neomycin to RRE. The three observed sites for neomycin binding to RRE are the tight binding, the intermediate affinity binding, and the very weak binding sites, showing K_D's of 250 nM, 1.9 μM, and 41 μM, respectively. In contrast, K_D of Rev binding to RRE is 20 nM [17]. Based on these results, it is clear that the tightest binding of neomycin to RRE is not inhibitory to Rev binding. Therefore, extensive effort to modify aminoglycoside antibiotics in order to

*Corresponding author
Phone: 82-2-3277-4653; Fax: 82-2-3277-2851;
E-mail: ykwon@ewha.ac.kr

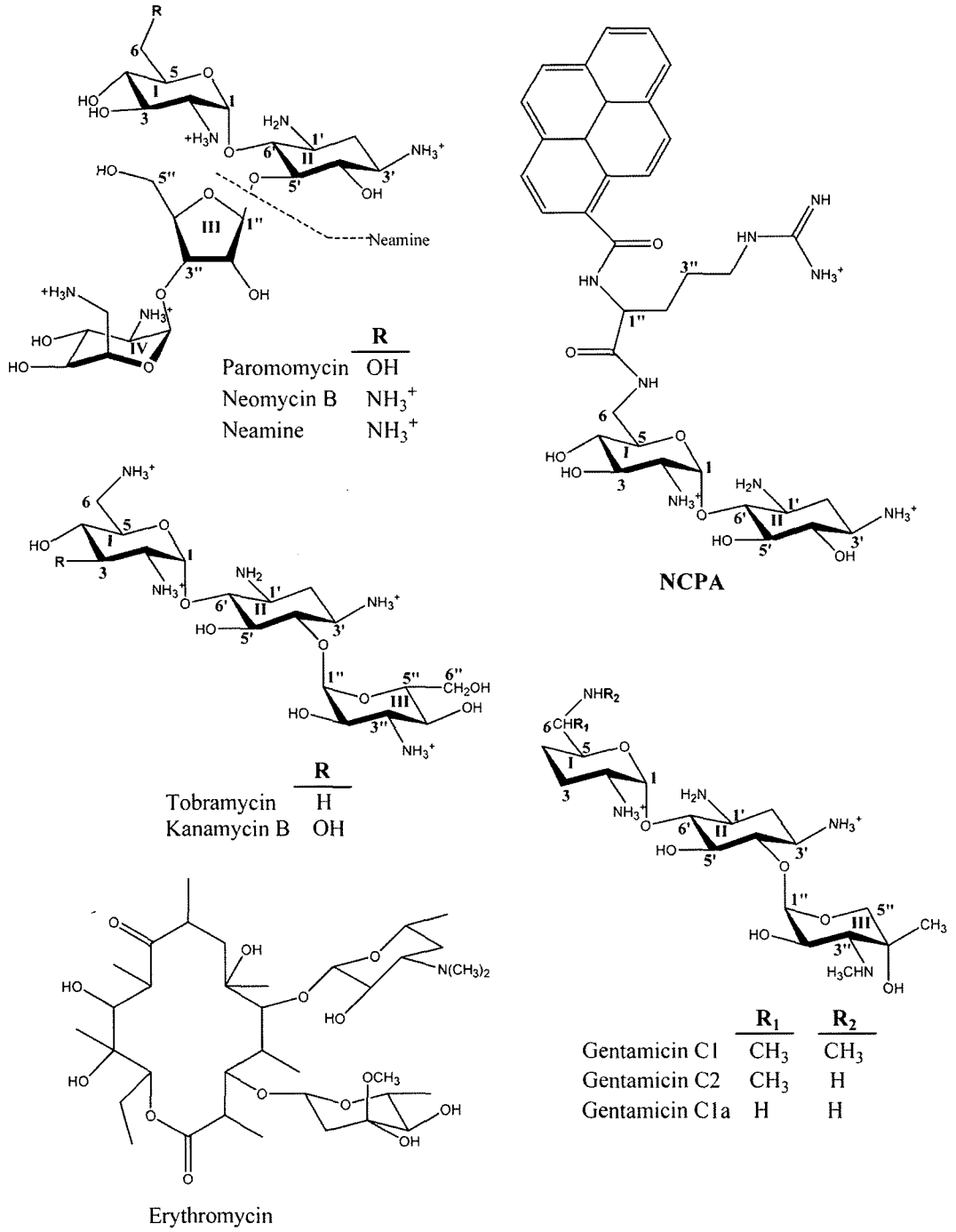

Fig. 1. The structures of aminoglycoside antibiotics used for UV experiments to screen the binding affinity to the RRE sequence.
Neamine contains rings I and II. The positively charged amino groups are based on each pK_a value [21], compared with pH 6.2 of NMR buffer solution.

enhance the ability to inhibit Rev binding to RRE has been attempted. The conjugation of acridine to neomycin and that of arginine, or arginine-pyrene to neamine, have been attempted [9, 17]. Tok *et al.* [32] confirmed that there was more than one neomycin-binding site on RRE by using dimeric neomycin synthesized, and they also showed a 17-fold enhancement of dimeric neomycin in K_D as compared with monomeric neomycin. In order to provide the basis for a more promising approach to develop a Rev-RRE binding inhibitor against HIV-1 infection, it is necessary to understand the binding modes of the aminoglycoside antibiotics to RRE and to elucidate the mechanism for the inhibition of Rev binding. The present study was undertaken to study the following questions; (1) what the structural

factors are for the aminoglycoside antibiotics to obtain the binding affinity to RRE and (2) how a modified antibiotic, NCPA, exhibits better binding affinity to RRE. The T_m measurement and spectroscopic analysis of RRE with or without antibiotics were employed to address these questions.

MATERIALS AND METHODS

Materials

Paromomycin sulfate was purchased from Fluka. Neomycin, tobramycin sulfate, gentamicin sulfate, kanamycin B sulfate, and erythromycin were purchased from Sigma. The DNA templates were synthesized using the standard β-cyanoethyl phosphoramidite method on an Expedite 8900 DNA synthesizer (Perseptive Biosystems, Framingham, MA, U.S.A.). DNA was purified by HPLC (reverse-phase C_{18} prep-column) and desalted (Bio-Rad Econo-Pac 10 DG). The purity of the sample was examined using reverse-phase C_{18} HPLC and electrophoresis on 20% denaturing polyacrylamide gel. The sequences of the top-strand and template-strand DNA molecules were: top, 5'-TAATACGACTCACT-ATAG-3': template, 5'-GGTGTACCGTCAGCCGAAGCTGCGC-CCACCTATAGTGA-GTCGTATTA-3'. All NTPs were purchased from Pharmacia LKB Biotechnology. T7 RNA polymerase was purified as described by Milligan *et al.* [24]. NCPA (Fig. 1), generously supplied by Dr. Hamasaki, Waseda University in Japan, was purified by HPLC (reverse phase C-8 semiprep column, Waters, Milford, MA, U.S.A.) with a gradient mobile phase formed from 17% A-83% B (solvent A: 0.1 % TFA in CH_3CN; solvent B: 0.1% TFA in H_2O) to 30% A-70% B within 40 min. The purity of NCPA was checked by HPLC and Maldi-TOF mass spectrometery (proFLEX III, Bruker Daltonics). A sharp single peak on HPLC and two peaks of 707.264 m/z $[M+H^+]$ and 729.288 m/z $[M+Na^+]$ from mass spectrum were obtained, confirming that the synthesized NCPA product was pure.

Sample Preparation

RRE3 Design, Synthesis, and Purification. RRE is localized in the envelope sequences of the HIV-1 RNA genome and consists of a 234-nucleotide (nt) RNA that forms an array of stem loops [10, 22]. The stem-loop IIB domain has been reported to be sufficient for high affinity Rev binding *in vivo* and *in vitro* [33]. Surprisingly, this binding core of 45–54:64–75 regions in the stem-loop IIB domain is highly conserved. For the reverse transcription, such as the HIV-1 viral replication, highly frequent mutation is expected because of its lack of a proofreading step. The naturally less frequent mutation in this Rev-binding core of RRE was confirmed by the sequence alignments using the HIV database. The nine residues of G55-C63 are not critical for the Rev binding ability. In this regard, in order to enhance the stability of the hairpin structure in the binding core, a tetra-loop of UUCG was introduced in place of G55-C63 residues. A 30-nt sequence named RRE3 (Fig. 2) is originated from the stem-loop IIB domain and contains most conserved residues for fully binding to Rev [33]. The two consecutive GG residues were introduced for T7 polymerase transcription efficiency *in vitro*. RRE3 was prepared by *in vitro* T7 polymerase runoff transcription using synthesized oligonucleotide templates [25]. The small-scale transcription reactions were conducted prior to a scale-up reaction, since the optimal concentrations of NTPs, free Mg^{2+}, and T7 polymerase solutions strongly depend on the template sequence composition as well as the concentration of template. In the small-scale 1 ml reaction, 250 nM template was first pre-annealed to 250 nM primer by heating the mixture at 90°C for 2 min. After cooling down the mixed template and primer solution at room temperature, all transcription reaction buffers were carefully added, and then 0.6 mg of T7 RNA polymerase was finally added. The optimized concentrations of transcription reaction buffers were 15 mM $MgCl_2$, 40 mM TRIS (pH 8.0), 5 mM DTT, 0.01% Triton X-100, 80 mg/ml PEG, 2 mg/ml Ipp, 4 mM each of NTPs, and 2 mM spermidine. All reaction buffers must be added before the addition of T7 RNA polymerase. The reaction mixture was incubated at 42°C for three hours. The reaction mixture turned cloudy, indicating that the reaction was in progress. The RRE3 RNA was precipitated with ethanol and purified using denaturing gel electrophoresis. The gel used for purification contained 20% polyacrylamide (19:1, acrylamide:BIS) and 7 M urea. The bands were visualized by shadowing the gel with UV light over a fluorescent thin-layer chromatography plate, and the full-length product was cut out and eluted from the gel using the elution buffer containing 0.5 M NH_4Ac and 0.1 mM EDTA. The supernatant of the elution, separated from the gel by a centrifugation and a filtration through a 0.45 μm syringe filter (Millex-GP, Millipore), was collected (crush and soak method). The collected eluate was loaded on a Sep-pack column (Waters), eluted again by acetonitrile: methanol:H_2O (3.5:3.5:3.0) solution, and then lyophilized to a white pellet, RRE3 RNA. The sample was resuspended in the solution containing 10 mM sodium phosphate and 0.1 mM EDTA, pH 6.2, (unless otherwise indicated, this condition is referred to as NMR buffer solution) and extensively dialyzed against this NMR buffer using centricon ultrafiltration (Amicon, Cetricon YM-3; Millipore, 3000 MW cut-off). The two large-scale (10 ml) transcription reactions were carried out in the same manner as the small-scale reaction. The concentration of RRE3 RNA was found to be approximately 1.3 mM by measuring the absorbance of the sample solution at 260 nm using an extinction coefficient of 281,400 M^{-1} cm^{-1} [30]. The final RRE3 RNA solution of 300 μl was kept in a freezer (−47°C) in a completely lyophilized state until use.

Preparation of NCPA-RRE3 Complex. The free RNA was dissolved in NMR buffer solution. NCPA dissolved in H_2O (adjusted to pH 6.2) was gradually added at 295 K and the ^1H (proton)-NMR spectrum was recorded to monitor the formation of the complex. The formation of the complex generates new NMR signals and also shows chemical shift change, compared with original signals. The final NMR sample contained about 1 mM NCPA-RRE3 complex at pH 6.2.

UV Experiments

All experiments on UV T_m melting measurements were done with a Varian Cary 3E spectrometer. To obtain a direct comparison, all experiments were performed in parallel. The free RRE3 RNA sample (3.5 μM) was used after dilution with NMR buffer solution, which gave 0.5 to 0.6 absorbance readings at 260 nm in a 10-mm path length cell. The antibiotics were added in the same concentration as the RRE3 solution to form 1:1 ratio complexes. All antibiotics were dissolved in the NMR buffer solution, except for erythromycin and NCPA: Erythromycin was dissolved first in the NMR buffer:MeOH (1:1) solution, then diluted with only NMR buffer solution to obtain almost the same solvent condition as the rest of the sample solutions. NCPA was dissolved in water as a 10-fold concentration in order not to change the salt condition of the RRE3 solution when it was added. Prior to the experiment, the solution in the cell was degassed using a vacuum desiccator to eliminate an unknown spike due to the air in the sample. The temperature was changed from 0 to 90°C with a rate of 1.0°C/min. To avoid evaporation of solvent, mineral oil was used to cover the surface of the sample solution. Three to six trials of complete cycle measurements (heating and annealing the sample) were performed for each sample, and the T_m value was then calculated using a Microsoft Excel program, developed in Dr. Gao's laboratory [40].

NMR Experiments

All NMR experiments were performed on a Bruker AMX-II and AVANVCE 600 MHz spectrometer at the Department of Chemistry, University of Houston. The spectra of the samples were recorded in 90% H_2O and 10% D_2O (Cambridge Isotopes Inc.) for observing exchangeable protons and 99.99% D_2O for observing non-exchangeable protons. Proton chemical shifts were referenced to the HOD resonance (4.70 ppm at 25°C, temperature correction factor - 0.0109 ppm/°C). The ^{31}P chemical shifts were referenced to the signal of an external sample containing trimethyl phosphate in 0.1 M sodium phosphate, pH 6.3, at 298 K. One-dimensional (1D) ^1H-NMR spectra (25 ppm spectral window and 8 K total data points for H_2O samples and 10 ppm spectral window and 4 K total data points for D_2O samples) were collected at the temperature range from 273 to 303 K to find the critical temperature, showing the well-resolved exchangeable and non-exchangeable protons. The Jump-Return (J-R) pulse sequence (90_x-τ-90_{-x}-Acq) [27] was used for the H_2O sample to obtain efficient water suppression with a refocusing delay of 52 μs, whereas the presaturation pulse was used for D_2O samples. The 1D ^{31}P-NMR spectra were recorded with a spectral width of 5 ppm and total data points of 8 K. For two-dimensional (2D) ^1H-^1H-NMR spectra, the parameters used in 1D experiments were accepted, but data points in t2 were half of that used for 1D spectra (for samples in D_2O, acquisition time was 682 ms for COSY type of spectra, and 341 ms for NOESY; for samples in H_2O, acquisition time was 158 ms) and were 512 in t1 (for samples in D_2O, $t1_{max}$=171 ms; for samples in H_2O, $t1_{max}$=79 ms). The 2D ^1H-^{31}P correlation spectra used a sweep width of 3.3 ppm in t2 (^1H) and 4.6 ppm in t1 (^{31}P), and the acquisition times were 512 and 133 μs for the ^1H and ^{31}P dimensions, respectively. The spectra were processed using the FELIX 2000 program (Accelrys Inc., Madison, WI, U.S.A.) and the XWIN-NMR program (Bruker Instruments Inc., Billerica, MA, U.S.A.). NOESY processing used a 90° phase-shifted sine bell in both t_2 and t_1 dimensions prior to Fourier transformation; TOCSY and DQF-COSY processing used a 30° phase-shifted skewed sine bell; ^1H-^{31}P processing used a 37.5° phase-shifted skewed sine bell function. The final spectral matrices had 2,048×2,048 data points for 2D ^1H-^1H-NMR spectra, and 1,024×1,024 data points for ^1H-^{31}P spectra. The 2D J-R NOESY spectra were recorded in 90% H_2O-10% D_2O buffer solutions (200 and 300 ms mixing times; 0.9 s repetition delay for NCPA-RRE3 complex and 0.9 s relaxation delay; 150, 300 ms mixing times for free RRE3 RNA) at 285 and 295 K. 2D NOESY spectra of free RRE3 and bound RRE3 to NCPA for observing non-exchangeable protons were acquired at 288 and 303 K (4 s repetition delay; 70, 250, and 500 ms mixing times). DQF-COSY, COSY-35, and TOCSY, and ^1H-^{31}P correlation spectra of free RRE3 and bound RRE3 to NCPA were obtained at 303 K. The 2D DQF-COSY and TOCSY (80 and 100 ms mixing times) of free NCPA were recorded with a 3 s relaxation delay at 283 and 295 K.

RESULTS AND DISCUSSION

T_m vs Binding Affinities of Antibiotics

The unique characteristic of aminoglycoside antibiotics, having the positively charged amino groups in their structure (Fig. 1), appears to play an important role in binding to RRE, since the arginine-rich region of the Rev protein interacts to RRE with high affinity [17, 38]. The electrostatic interaction of the positively charged amino group with RRE has been known as one of the important factors in binding affinity. In order to monitor the stability of RRE3

Table 1. Results of UV thermal melting studies.[a]

Samples	T_m (°C)	ΔG^b (Kcal/mol)	ΔH (Kcal/mol)	ΔS (cal/mol)	Hyperchromicity (%)
Free RRE	57.2	-11.5	-57.7	-149.0	19.5
RRE+Neomycin	**81.8**	**-28.2**	**-66.8**	**-163.2**	**13.9**
RRE+Paromomycin	73.9	-13.7	-54.4	-133.7	11.0
RRE+Tobramycin	70.4	-13.3	-56.5	-139.4	11.2
RRE+Kanamycin	76.1	-15.9	-70.6	-176.4	11.3
RRE+Gentamicin	73.0	-15.3	-69.4	-173.4	10.7
RRE+Erythromycin	58.9	-11.4	-54.2	-138.0	13.2
RRE+NCPA	**83.7**	**-19.7**	**-92.4**	**-234.6**	**13.3**

[a]These data are the average of the curve fitting results from three to six trials of complete thermal heating and cooling cycles.
[b]The value of ΔG was derived for 310 K.

on forming a complex with antibiotics, the T_m of RRE3 was measured with each of the aminoglycoside antibiotics. The calculated T_m and thermodynamic parameters derived are summarized in Table 1. The T_m of the combined erythromycin with RRE3 was essentially the same as that of free RRE3. This would be expected, since its structure does not possess the amino groups necessary for inducing an electrostatic interaction with RRE3. Introduction of a hydroxyl group on paromomycin instead of an amino group on neomycin produced a severe change in T_m, from 81.8 to 73.9°C. Each of paromomycin, tobramycin, and kanamycin B has five amino groups. The T_m values ranged from 70.4 to 76.1°C, indicating that there is some structural difference due to the presence of a furanose ring in some cases. The presence of one more hydroxyl group in the kanamycin B caused almost six degrees increase of T_m, compared with tobramycin. It appears that hydrogen bonds involving amino and hydroxyl groups of the antibiotics could contribute to the recognition of the RRE3 RNA. Interestingly, when gentamicin was combined with RRE3, it gave 73°C of T_m. Gentamicin is a mixture of C1, C2, and C1a (Fig. 1). In structural comparison, gentamicin has at least one amino group less (in the case of C1a) and two hydroxyl groups less than tobramycin. However, the addition of gentamicin solution to RRE gave three degrees higher T_m than that of tobramycin. These results imply that there should be additional weak interactions between the antibiotics and RRE that discriminate between cognate RNA aptamers. Further investigation on the complex of RRE-gentamicin at the molecular level would explain the specificity of antibiotic binding to HIV-1 RNA. NCPA introduced a slightly higher T_m increase than neomycin did (Table 1). The melting curve pattern of RRE3 with NCPA was similar to that of RRE3 with neomycin (Fig. 1). NCPA consists of three functional groups; a pyrene ring, an arginine chain, and neamine. The neamine is the conserved two rings in most aminoglycoside antibiotics and the best core in their series according to assays for *in vitro* RNA binding and antibiotic activity [9]. Arginine is the richest amino acid in the high RRE-binding domain of the Rev peptide [2, 3] and has a unique structural feature called arginine fork alignment; guanidinium ion can easily generate a specific interaction with the negatively charged nucleic acid backbone because of its positive charge and plane surface [4]. About 2°C higher T_m of RRE3 in the presence of NCPA than that of RRE3 with neomycin is consistent with the result that NCPA binds with an equivalent binding affinity as Rev (K_d=8.5 nM) [19]. In addition, the higher T_m of RRE3 in the presence of NCPA indicates that NCPA should be a good inhibitor for Rev binding to RRE; however, further investigation is necessary to verify whether its tight binding site is an inhibitory site.

Spectral Analysis of RRE3-NCPA Complex

Titration of the free NCPA to the RRE3 solution was carried out at 295 K. When concentrated NCPA solution was added, a white cloudy precipitate appeared. This precipitation was most likely formed by EDTA salt in the buffer solution that affects the NCPA solubility. All assigned proton chemical shifts of NCPA and RRE as a complex

Table 2. ^{1}H Chemical shifts of the complexed NCPA to RRE3.[a]

Arginine fragment					
H1"	H2"1/H2"2	H3"1/H3"2	H4"1/H4"2		
4.64	1.92/1.98	1.79/1.79	3.25/3.25		
4.58	1.92/1.96	1.81/1.81	3.25/3.25		
Ring I					
H1	H2	H3	H4		
5.73	3.26	3.90	3.44		
5.71	3.37	3.97	3.47		
Ring II					
H1'	H2'1/H2'2	H3'	H4'	H5'	H6'
3.14	1.65/2.12	3.28	3.78	3.57	3.45
3.04	1.50/2.25	3.28	3.61	3.63	3.49

[a]Non-exchangeable ^{1}H chemical shifts are obtained from spectra collected at 295 K.

Table 3. ^{1}H Chemical shifts of the complexed RRE to NCPA.[a]

DNA	H6/H8	H2/H5	H1'	imino
G1	8.07		5.79	
G2	7.53		5.87	13.25
U3	7.63	5.10	5.50	13.68
G4	7.59		5.64	
G5	7.71		5.70	
G6				
C7	7.75	5.45		
G8	7.55		5.73	
C9	7.55	5.34	5.32	
A10	7.96	6.94	5.79	
G11	7.22		5.58	13.40
C12	7.34	5.09	5.43	
U13	7.71	5.66	5.63	11.62
U14	7.99	5.82	6.05	
C15	7.65	6.09	5.92	
G16	7.82		5.92	9.83
G17	8.07		4.91	13.32
C18	7.62	5.25	5.25	
U19	7.75	5.45	5.50	13.70
G20	7.71		5.70	12.01
A21	8.09		5.97	
C22	7.38	5.28	5.28	
G23	7.47		5.65	
G24	7.66		5.59	
U25	7.83	5.77	5.92	
A26	8.12	5.24	5.81	
C27	7.58	5.40	5.25	
A28	8.01	7.34	5.86	
C29	7.47	5.15	5.37	
C30	7.58	5.40	5.72	

[a]Non-exchangeable ^{1}H chemical shifts are mainly from the spectrum collected at 303 K with 500 ms mixing time. Exchangeable ^{1}H chemical shifts are from the spectrum recorded at 288 K with 300 ms mixing time. The sample was dissolved in the solution containing 10 mM phosphate and 0.1 mM EDTA, pH 6.2.

form are summarized in Table 2 and 3, respectively. The assignments of exchangeable and non-exchangeable protons have been obtained from analyses of 2D NOESY, DQF-COSY, TOCSY, and J-R NOESY spectra collected at different temperatures in H_2O and D_2O, in comparison with data previously published [17, 27, 28]. The very strong scalar coupled peak between H1" and H2"1/H2"2 of NCPA (Hα and Hβ methylene protons) were observed in the DQF-COSY spectrum at ~4.6 ppm (F2) and ~1.92/1.98 ppm (F1). The long-range couplings through bonds of H3"1/H3"2 and H4"1/H4"2 protons in the TOCY spectrum were also obtained. Combined results of these two sets of ^{1}H chemical shifts of NCPA from the NMR experiments and one peak of NCPA by HPLC suggest that ten chiral centers in ring I and II of neamine, and one chiral center at Cα carbon, made NCPA exist as diastereomers in the solution. The pyrene ring protons of NCPA could not be assigned,

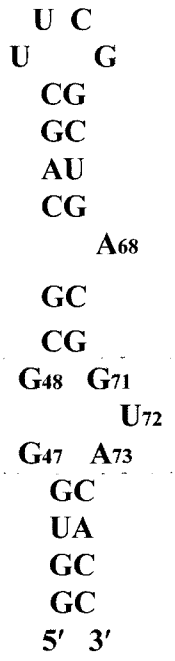

Fig. 2. RRE3 RNA sequence of the truncated 30-nt RNA hairpin derived from the RRE stem-loop IIB hairpin domain.
Two G residues in the 5' end are launched for efficiency of T7 polymerase *in vitro* transcription. The 5'-UUCG tetra-loop was introduced because of its structural stability in the loop. However, this 30-nt sequence still binds to Rev as much as the wild-type of the RRE IIB domain. The most important nucleotides for Rev binding are in the shaded box. The numbers of residues are employed from the wild-type of RRE IIB.

because of no specific intra-NOE peak, no unique spin system, and severe overlapping; four protons at 7.61 ppm, three at 7.20 ppm, one at 8.22 ppm, and one at 8.45 ppm in the complex form. However, two clusters of the pyrene protons detected at 7.20 and 7.61 ppm were upfield shifted from 7.81 and 8.01 ppm in the free form, respectively. The upfield shifted resonances of pyrene protons confirm the pyrene ring intercalating into the internal loop and stacking above or below the base pair. The changes in chemical shifts of RRE3 imino protons (NHs) were monitored. The change pattern in chemical shifts of RRE3 NHs upon the complex formation was similar to that of RRE bound to Rev (data not shown), implying that the NCPA binding directly competes for the Rev binding to RRE [27]. The base proton-H1' region of the NOESY spectrum of RRE3 at 303 K is shown in Fig. 3. Ambiguities in the assignments due to severe spectral overlap have been resolved by comparison of spectra obtained at different temperatures and previously published data [27, 28]. Owing to the small H1'-H2' coupling constants for RNA, a few H1'-H2' cross-peaks have been obtained in DQF-COSY and TOCSY spectra. The very weak or absent sequential connection of G5-G6-C7-G8 and U25-A26-C27 indicates an internal loop region. The intensity of the H8-H1' cross-peak of G16 and G24 residues in the free RRE3 was comparable to that of

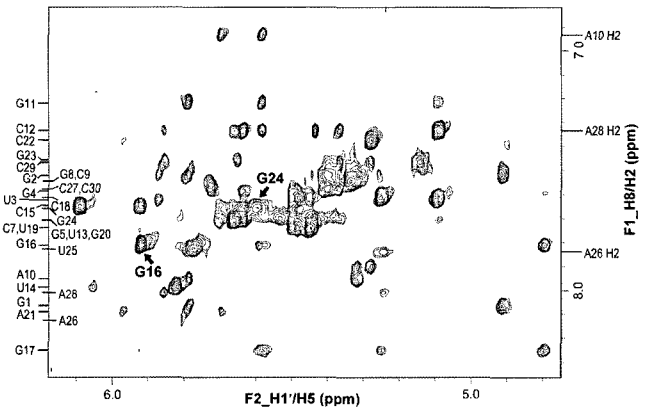

Fig. 3. Base-H1' proton region of a NOESY spectrum (500 ms mixing time) of the RRE3-NCPA complex recorded in D_2O at 303 K.
The H8-H1' cross-peaks of G16 and G24 residues are arrow-marked.

the H6-H5 cross-peak of a pyrimidine residue in the short mixing time (70 ms) NOESY spectrum, which supports the hypothesis that these G16 and G24 nucleotides adopt a *syn*-type configuration in their glycosidic bonds in the free form. However, the H8-H1' cross-peak of the complexed G24 to NCPA disappeared in the 70 ms mixing time NOESY spectrum, while that of G16 remained highly intense. The H8-H1' cross-peaks of G16 and G24 residues in the RRE3-NCPA complex are arrow-marked in Fig. 3. The H8-H1' cross-peak of G24 in the form of complex was not as strong as G16, even in the 500 ms mixing time NOESY spectrum. It was previously observed that the non-Watson-Crick base pair of G48:G71 in the internal loop had a critical role for being recognized by the Rev protein, in spite of no specific interactions between the G48:G71 mismatched base pair and Rev. The conformational transition of G71, from *syn* to *anti* upon complex formation with Rev, causes the RRE major groove to open and allows for Rev binding [12, 14]. The G24 residue in RRE3 corresponds to G71 in the RRE IIB region. The base of G24 adopted the same conformational change upon binding to NCPA as G71 change by complexing with Rev. The correlation between phosphorus and the sugar protons of H3', H4', and H5'/H5" were obtained from the ^{1}H-^{31}P-COSY spectrum (data not shown). The broad dispersion in ^{31}P dimension (>2.5 ppm) implies a typical characteristic of noncanonical RNA. These spectroscopic results as well as K_d of NCPA to RRE and T_m of RRE3 in the presence of NCPA support the notion that NCPA directly competes against Rev for binding to the RRE internal loop region.

Implications for Drug Design

Structures of aminoglycoside antibiotics, including neomycin [23], paromomycin [18, 20], and gentamicin [37], complexed with diverse RNAs were obtained from a protein databank and comprehensively reviewed. It is worthy to note the general tendency of aminoglycoside antibiotics to achieve high binding affinity for the target RNA sequences; ring II is the most conservative moiety among the diverse aminoglycoside antibiotics. Ring II was not modified in diverse aminoglycoside antibiotics. Rings II and III anchor inside the binding pocket generated by extra none-paired one or more base(s). In ring I, two hydroxyl protons at C3 and C4 and amino proton at C6 play a critical role to have electrostatic interaction with RRE RNA by positioning next to the RNA backbone. Specifically, the hydroxyl at C3 forms a direct hydrogen bond with the anionic phosphate oxygen of RNA. That is the reason why T_m of tobramycin is lower than those of neomycin, paromomycin, and kanamycin B. In ring III, the C2"-hydroxyl proton generally forms a hydrogen bond with the base pair of RNA, and C4" and C6" hydroxyl groups are not in hydrogen bond contact with RNA. The T_m difference between tobramycin and gentamicin gives a clue that the hydrophobic interaction by ring III, especially by aliphatic protons at C4", C5", and C6", may enhance the binding affinity. Based on the experimental results in the present study and review of the structures of antibiotic complexes with diverse RNA sequences, a key driving force in the binding of aminoglycoside to RNA appears to be the electrostatic interaction between the positively charged ammonium groups of aminoglycoside antibiotics and the negatively charged RNA. However, the number of contacts through hydrogen bonds and hydrophobic interaction in the binding pocket may also control high binding affinity with specificity to certain RNA sequences. Therefore, such structures modified as follows would serve as a good antiviral drug candidate; (1) the replacement of amide possessing a planar moiety with amine at C6 in ring I, (2) no change in ring II, and (3) a slightly longer aliphatic chain at C4", C5", and/or C6" of ring III. The fermentation engineering technology may hopefully utilize these structural implications to develop new generation of antibiotics [5, 15, 31, 39].

Acknowledgments

This study was financially supported by the Ewha Womans University Research Grant of 2004. NCPA is a generous gift from Dr. Hamasaki, Waseda University, Japan.

References

1. Barre-Sinoussi, F., J. C. Chermann, F. Rey, M. T. Nugeyre, S. Chamaret, J. Gruest, C. Dauguet, C. Axler-Blin, F. Vezinet-Brun, C. Rouzioux, W. Rozenbaum, and L. Montagnier. 1983. Isolation of a T-lymphotropic retrovirus from a patient at risk for acquired immune deficiency syndrome (AIDS). *Science* **220:** 868–871.

2. Battiste, J. L., H. Mao, S. Rao, R. Tan, D. R. Muhandiram, L. E. Kay, A. D. Frankel, and J. R. Williamson. 1996. α Helix-RNA major groove recognition in an HIV-1 Rev peptide-RRE RNA complex. *Science* **273:** 1547–1551.
3. Battiste, J. L., R. Tan, A. D. Frankel, and J. R. Williamson. 1994. Binding of an HIV Rev peptide to Rev responsive element RNA induces formation of purine-purine base pairs. *Biochemistry* **33:** 2741–2747.
4. Calnan, B. J., B. Tidor, S. Biancalana, D. Hudson, and A. D. Frankel. 1991. Arginine-mediated RNA recognition: The arginine fork. *Science* **252:** 1167–1171.
5. Cho, B.-G., C.-H. Kim, B. K. Lee, and S.-H. Cho. 2005. Comparison of antibiotics resistance of blood culture strains and saprophytic isolates in the presence of biofilms, formed by the intercellular adhesion (ica) gene cluster in *Staphylococcus epidermidis*. *J. Microbiol. Biotechnol.* **15:** 728–733.
6. Cochrane, A. W., C. H. Chen, and C. A. Rosen. 1990. Specific interaction of the human immunodeficiency virus Rev protein with a structured region in the env mRNA. *Proc. Natl. Acad. Sci. USA* **87:** 1198–1202.
7. Emerman, M., R. Vazeux, and K. Peden. 1989. The rev gene product of the human immunodeficiency virus affects envelope specific RNA localization. *Cell* **57:** 1155–1165.
8. Felber, B. K., M. Hadzopoulou-cladaras, C. Cladaras, T. Copeland, and G. N. Pavlakis. 1989. Rev protein of human immunodeficiency virus type 1 affects the stability and transport of the viral mRNA. *Proc. Natl. Acad. Sci. USA* **86:** 1495–1499.
9. Greenberg, W. A., E. S. Priestley, P. S. Sears, P. B. Alper, C. Rosenbohm, M. Hendrix, S.-C. Hung, and C.-H. Wong. 1999. Design and synthesis of new aminoglycoside antibiotics containing neamine as an optimal core structure: Correlation of antibiotic activity with *in vitro* inhibition of translation. *J. Am. Chem. Soc.* **121:** 6527–6541.
10. Hamasaki, K. and A. Ueno. 2001. Aminoglycoside antibiotics, neamine and its derivatives as potent inhibitors for RNA-protein interactions derived from HIV-1 activators. *Bioorg. Med. Chem. Lett.* **11:** 591–594.
11. Hendrix, M., S. Priestly, G. F. Joyce, and C. H. Wong. 1997. Direct observation of aminoglycoside-RNA interactions by surface plasmon resonance. *J. Am. Chem. Soc.* **119:** 3641–3648.
12. Hung, L.-W., E. L. Holbrook, and S. R. Holbrook. 2000. The crystal structure of the Rev binding element of HIV-1 reveals novel base pairing and conformational variability. *Proc. Natl. Acad. Sci. USA* **97:** 5107–5112.
13. Icacmpo, S. and A. Cochrane. 1996. Human immunodeficiency virus type 1 Rev function requires continued synthesis of its target mRNA. *J. Virol.* **70:** 8332–8339.
14. Ippolito, J. A. and T. A. Steitz. 2000. The structure of the HIV-1 RRE high affinity Rev binding site at 1.6 Å resolution. *J. Mol. Biol.* **295:** 711–717.
15. Kharel, M., B. Subba, H. C. Lee, K. Liou, J. S. Woo, D. H. Kim, Y.-H. Moon, and J. K. Sohng. 2003. Identification of 2-deoxy-scyllo-inosose synthase in aminoglycoside producer *Streptomyces*. *J. Microbiol. Biotechnol.* **13:** 828–831.
16. Kirk, S. R., N. W. Leudtke, and Y. Tor. 2000. Neomycin-acridine conjugate: A potential inhibitor of Rev-RRE binding. *J. Am. Chem. Soc.* **122:** 980–981.
17. Lacourciere, K. A., J. T. Stivers, and P. Marino. 2000. Mechanism of neomycin and Rev peptide binding to Rev responsive element of HIV-1 as determined by fluorescence and NMR spectroscopy. *Biochemistry* **39:** 5630–5641.
18. Lapidot, A., V. Vijayabaskar, A. Litovchick, J. Yu, and T. L. James. 2004. Structure-activity relationships of aminoglycoside-arginine conjugates that bind HIV-1 RNAs as determined by fluorescence and NMR spectroscopy. *FEBS Lett.* **577:** 415–421.
19. Luedtke, N. W., Q. Liu, and Y. Tor. 2003. RNA-ligand interactions: Affinity and specificity of aminoglycoside dimers and acridine conjugates to the HIV-1 Rev response element. *Biochemistry* **42:** 11391–11403
20. Lynch, S. R., R. L. Gonzalez, and J. D. Puglisi. 2003. Comparison of X-ray crystal structure of the 30S subunit-antibiotic complex with NMR structure of decoding site oligonucleotide-paromomycin complex. *Structure (Camb.)* **11:** 43–53.
21. Malim, M. H., J. Hauber, S.-Y. Le, J. V. Maizel, and B. R. Cullen. 1989. The HIV-1 trans-activator acts through a structured target sequence to activate nuclear export of unspliced viral mRNA. *Nature* **338:** 254–257.
22. Malim, M. H., L. S. Tiley, D. F. McCarn, J. R. Rusche, J. Hauber, and B. R. Cullen. 1990. HIV-1 structural gene expression requires binding of the Rev trans-activator to its RNA target sequence. *Cell* **60:** 675–683.
23. Mikkelsen1, N. E., K. Johansson, A. Virtanen, and L. A. Kirsebom. 2001. Aminoglycoside binding displaces a divalent metal ion in a tRNA-neomycin B complex. *Nat. Struct. Biol.* **8:** 510–514.
24. Milligan, J. F., D. R. Groebe, G. W. Witherell, and O. C. Uhlenbeck. 1987. Oligoribonucleotide synthesis using T7 RNA polymerase and synthetic DNA templates. *Nucleic Acids Res.* **15:** 8793–8798.
25. Milligan, J. F. and O. C. Uhlenbeck. 1989. Synthesis of small RNAs using T7 RNA polymerase. *Methods Enzymol.* **180:** 51–62.
26. Olsen, H. S., P. Nelbock, A. W. Cochrane, and C. A. Rosen. 1990. Secondary structure is the major determinant for interaction of HIV rev protein with RNA. *Science* **247:** 845–848.
27. Peterson, R. D., D. P. Bartel, J. W. Szostak, S. J. Horvath, and J. Feigon. 1994. ^{1}H NMR studies of the high-affinity Rev binding site of the Rev Responsive Element of HIV-1 mRNA: Base pairing in the core binding element. *Biochemistry* **33:** 5357–5366.
28. Peterson, R. D. and J. Feigon. 1996. Structural change in Rev Responsive Element RNA of HIV-1 on binding Rev peptide. *J. Mol. Biol.* **264:** 863–877.
29. Plateau, P. and M. Guéron. 1982. Exchangeable proton NMR without base-line distortion, using new strong-pulse sequences. *J. Am. Chem. Soc.* **104:** 7301–7311.
30. Puglish, J. D. and I. Jr. Tinoco. 1989. Absorbance melting curves of RNA. *Methods Enzymol.* **180:** 304–325.

31. Rhee, K. Y. 2003. Purification and identification of an antifungal agent from *Streptomyces* sp. KH-614 antagonistic to rice blast fungus *Pyricularia oryzae*. *J. Microbiol. Biotechnol.* **13:** 984–988.
32. Tok, J., L. J. Dunn, and R. C. Des Jean. 2001. Binding of dimeric aminoglycosides to the HIV-1 Rev responsive element (RRE) RNA construct. *Bioog. Med. Chem. Lett.* **11:** 1127–1131.
33. Tuerk, C. and S. MacDougal-Waugh. 1993. *In vitro* evolution of functional nucleic acids: High-affinity RNA ligands of HIV-1 proteins. *Gene* **137:** 33–39.
34. Turner, B. G. and M. F. Summers. 1998. Structural biology of HIV. *J. Mol. Biol.* **285:** 1–32 and references therein.
35. Van Ryk, D. I. and S. Venkatesan. 1999. Real-time kinetics of HIV-1 Rev-rev responsive element interactions. Definition of minimal binding sites on RNA and protein and stoichiometric analysis. *J. Biol. Chem.* **274:** 17452–17463.
36. Wei, X., S. K. Ghosh, M. E. Taylor, V. A. Johnson, E. A. Emini, P. Deutsch, J. D. Lifson, S. Bonhoeffer, M. A. Nowak, B. H. Hahn, M. S. Saag, and G. M. Shaw. 1995. Viral dynamics in human immunodeficiency virus type 1 infection. *Nature* **373:** 117–122.
37. Yoshizawa, S., D. Fourmy, and J. D. Puglisi. 1998. Structural origins of gentamycin antibiotic action. *EMBO J.* **17:** 6437–6448.
38. Zapp, M. L. and M. R. Green. 1989. Sequence-specific RNA binding by the HIV-1 Rev protein. *Nature* **342:** 714–716.
39. Zhao, X.-Q., K.-R. Kim, L. W. Sang, S.-H. Kang, Y.-Y. Yang, and J.-W. Suh. 2005. Genetic organization of a 50-kb gene cluster isolated from streptomyces kanamyceticus for kanamycin biosynthesis and characterization of kanamycin acetyltransferase. *J. Microbiol. Biotechnol.* **15:** 346–353.
40. Zheng, M., H. Huang, G. K. Smith, X. Yang, and X. Gao. 1996. Genetically unstable CXG repeats are structurally dynamic and have a high propensity for folding. An NMR and UV spectroscopic study. *J. Mol. Biol.* **264:** 323–336.